Correlation-based distributed measurement of a dynamic grating spectrum generated in stimulated Brillouin scattering in a polarization-maintaining optical fiber

Weiwen Zou,[1,*] Zuyuan He,[1,3] Kwang-Yong Song,[2] and Kazuo Hotate[1]

[1]*Department of Electrical Engineering and Information Systems, The University of Tokyo, Tokyo 113-8656, Japan*
[2]*Department of Physics, Chung-Ang University, Seoul 156-756, Korea*
[3] *zhe@ee.t.u-tokyo.ac.jp*
**Corresponding author: zou@sagnac.t.u-tokyo.ac.jp*

Received January 9, 2009; revised February 24, 2009; accepted February 24, 2009;
posted March 6, 2009 (Doc. ID 106149); published March 31, 2009

We study the principle of correlation-based distributed generation and readout of dynamic grating spectrum generated in stimulated Brillouin scattering in a polarization-maintaining optical fiber. The experimental validation is demonstrated by applying synchronous sinusoidal frequency modulations to two orthogonally polarized laser sources that serve as the Brillouin pump–probe light and readout light of the dynamic grating, respectively. Temperature-induced opposite changes in the Brillouin frequency shift and in the birefringence-determined optical frequency deviation are clearly observed with 1.2 m spatial resolution and a 110 m measurement range. © 2009 Optical Society of America

OCIS codes: 060.2370, 290.5900, 190.2055, 060.2630.

Brillouin optical correlation-domain analysis (BOCDA) [1,2] characterized by approximately centimeter or even subcentimeter spatial resolution with random access ability provides a promising way to build smart materials and smart structures. In comparison, the pulse-based Brillouin optical time-domain analysis (BOTDA) has approximately m-order spatial resolution limited by the bandwidth of Brillouin gain spectrum (BGS) in optical fibers [3], although improvements were recently made to some extent [4]. Both BOCDA and BOTDA are based on the same sensing mechanism: the linear dependence of Brillouin frequency shift (BFS, ν_B) of BGS on strain and temperature (+0.04 MHz/$\mu\varepsilon$ and +1.1 MHz/°C, respectively) [5]. Owing to the dual sensitivity, all the Brillouin-based sensors share the same physical difficulty in discriminating the response to strain and that to temperature. To solve this difficulty, we proposed recently a novel method by evaluating the BFS ν_B in addition to the birefringence-determined frequency deviation ($f_{yx}=B/n_{\mathrm{eff}}^{*}f_0$ with B being the birefringence, n_{eff} being the effective refractive index, and f_0 being the optical frequency) in a polarization-maintaining optical fiber (PMF) [6]. The dynamic grating spectrum (DGS) generated in stimulated Brillouin scattering (SBS) with x-polarized pump and probe waves [7] is readout with a y-polarized wave to precisely measure the f_{yx} that is oppositely changed by strain and temperature as +0.90 MHz/$\mu\varepsilon$ and −55.8 MHz/°C, respectively [6].

In this Letter, we show that the dynamic grating can be localized in an arbitrary position along the PMF by using a correlation-based cw technique. A distributed measurement of the DGS is demonstrated with 1.2 m spatial resolution and 110 m measurement range. In experiment, temperature-induced changes in both the BFS ν_B of BGS and the frequency deviation f_{yx} of DGS are measured in heated segments cascaded along a 110 m PMF.

In a BOCDA system with a PMF as the test fiber, x linearly polarized pump and probe waves counterpropagate in the fiber. The frequency of the probe is downshifted against that of the pump to around the BFS to induce the SBS interaction. Moreover, both pump and probe waves are frequency modulated in a sinusoidal manner, which makes the optical power spectrum of the pump probe a double-peak profile on average. In this way, a series of correlation peaks are synthesized periodically along the fiber. At the correlation-peak position, the pump–probe optical frequency offset keeps constant because of the in-phase situation, and thus the SBS interaction is localized. On the contrary, at positions other than the correlation peaks, the frequency offset changes in terms of time owing to the off-phase condition. The position-dependent SBS interaction can be expressed by the pump–probe beat power spectrum distribution [$S(z)$] as schematically shown in Fig. 1(a) [8]. The distance from the correlation peak to the neighboring location where the $S(z)$ broadens twice as the BGS

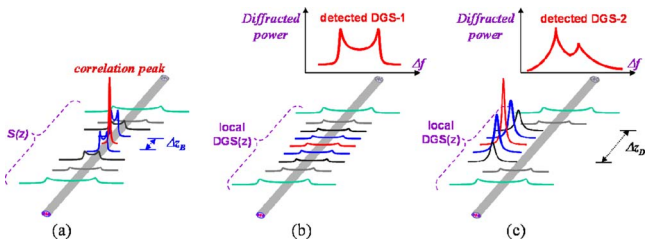

Fig. 1. (Color online) (a) Beat power spectrum distribution $S(z)$ near the correlation peak. The local DGS when the optical frequency of readout wave is (b) not modulated or (c) modulated synchronously to the modulation to pump light. The top plots show the measured DGS for (b) or for (c) when the correlation peak is localized in a heated segment.

linewidth ($\Delta\nu_B$) is defined as the BOCDA spatial resolution (Δz_B), and the correlation-peak interval is defined as the BOCDA measurement range (d_m) [8],

$$\Delta z_B = \frac{c}{2n_{\text{eff}}f_m}\frac{\Delta\nu_B}{\pi\Delta f}, \tag{1}$$

$$d_m = \frac{c}{2n_{\text{eff}}f_m}, \tag{2}$$

where c is the light speed in vacuum, Δf is the modulation depth, and f_m is the modulation frequency.

The DGS generated in SBS is readout with a y-polarized frequency-ramp-swept wave that is launched into the same fiber end as the x-polarized pump [6]. Since the sinusoidal FM is applied only to the x-polarized pump and probe, the frequency deviation between the pump and readout becomes time dependent and presents a double-peak profile as the same as the FM-induced optical power spectrum on average. Accordingly, the local DGS, which is given by the convolution of the local $S(z)$, the double-peak profile and the Gaussian-shaped intrinsic DGS, broadens not only at the uncorrelated positions but also at the correlation-peak position, as schematically illustrated in Fig. 1(b). As a result, the DGS has a double-peak profile and cannot represent the localized correlation peak.

To solve the above problem, we apply an additional sinusoidal FM to a y-polarized readout wave synchronous to that applied to an x-polarized pump with the same modulation depth Δf and modulation frequency f_m. Then, the frequency deviation between the pump and the readout is independent to the sinusoidal frequency modulation and is determined only by their central frequency difference. The synchronization means that the pump and readout waves experience in-phase modulations at any location of the PMF. In consequence, the local DGS becomes the convolution of the $S(z)$ and the Gaussian-shaped intrinsic DGS. The detected DGS, which is the integral of the local DGS, recurs as a Gaussian-like profile as depicted in Fig. 1(c) and is strongly related to the correlation peak. For the distributed measurement of DGS, the spatial resolution (Δz_D) becomes the distance from the correlation peak to the neighboring location where the $S(z)$ broadens twice as the intrinsic linewidth (Δf_{yx}) of the DGS as follows:

$$\Delta z_D = \frac{c}{2n_{\text{eff}}f_m}\frac{\Delta f_{yx}}{\pi\Delta f}. \tag{3}$$

The DGS linewidth Δf_{yx} was experimentally observed approximately ten times as the BGS $\Delta\nu_B$=30 MHz [6]. One possible explanation is due to the irregularity of the local birefringence, as will be shown below. Approximately, Δz_D is estimated as ten times the BOCDA spatial resolution Δz_B.

Figure 2 shows the experimental setup for distributed generation and detection of the DGS in an ~110 m long PMF (n_{eff}= ~1.446). The output from a 1549 nm distributed feedback laser diode (DFB-LD1)

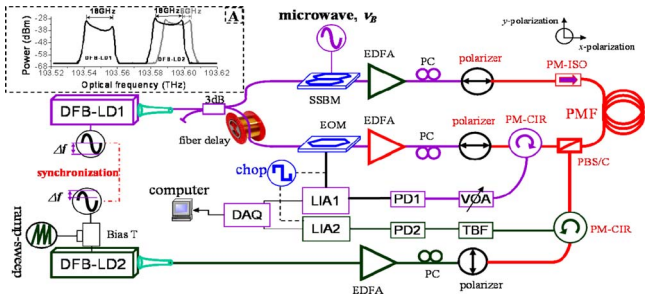

Fig. 2. (Color online) Experimental configuration for distributed generating and measuring the BGS and DGS in a PMF. The abbreviations are explained in the text body. Inset A depicts the optical power spectra of two modulated DFB-LDs both with $2\Delta f$=18 GHz, where the gray curve has 6 GHz offset from the black curve corresponding to a reduced dc injection current to DFB-LD2.

is equally divided into probe and pump beams. The probe beam is prepared by downshifting its frequency using a single-sideband modulator (SSBM) and a microwave synthesizer. It is amplified via an erbium-doped fiber amplifier (EDFA) and launched into the PMF after passing through an x polarizer and a polarization-maintaining isolator (PM-ISO). The pump beam is chopped by an electro-optic modulator (EOM) and amplified by a high-power EDFA, which is launched into the other end of the PMF after passing through an x polarizer, a PM circulator (PM-CIR), and a PM beam splitter–combiner (PBS–C). Used as the readout beam, the output from the second laser diode (DFB-LD2) is launched into the PMF after passing through a y polarizer and the PBS–C to readout the SBS-generated DGS. The frequency of the readout beam is deviated by f_{yx} from the pump beam by tuning the DFB-LD2's DC injection current. In experiment, the frequency deviation f_{yx} is ramp swept from 41 to 47 GHz, because the PMF's birefringence is $B=3.3\times10^{-4}$ and the corresponding central f_{yx0} =43.876 GHz [6]. A variable optical attenuator (VOA) and a tunable bandpass filter (TBF) placed in front of the photodetectors (PDs) are used to overcome the power saturation and to eliminate the x-polarized light leakage, respectively. The PD outputs are demodulated via lock-in amplifiers (LIAs) and recorded by a data acquisition card (DAQ) and a personal computer.

The FMs of both DFB-LDs are employed by direct current modulation with signal generators. Their optical spectra (see inset A of Fig. 2) show that the same modulation depths ($2\Delta f$=18 GHz) are applied. In the inset, an example is plotted when the center frequency of DFB-LD2 is detuned by 6 GHz through adjusting its dc current. The modulation frequency f_m is set around 930 kHz corresponding to a measurement range d_m>110 m according to Eq. (2). To scan a nonzeroth correlation peak, a fiber delay (~1.5 km) is introduced into the pump arm. The pump, probe, and readout powers are maximized via polarization controllers (PCs) and measured before entering the PMF as 25.0, 1.5, and 23.7 dBm, respectively.

At first, we experimentally confirmed the principles explained in Fig. 1. When no FM is applied to

DFB-LD2 while FM with different modulation depth is introduced to DFB-LD1, the measured DGS exhibits a double-peak profile as shown in Fig. 3(a). The double peaks separate more for greater modulation depths. When synchronously controlled FMs with $\Delta f = 9$ GHz and $f_m = \sim 930$ kHz are introduced to both lasers, $\Delta z_B = \sim 12$ cm and $\Delta z_D = \sim 120$ cm are estimated via Eqs. (1) and (3). Figure 3(b) summarizes the measured DGS of a heated PMF segment located at the correlation peak but with various lengths. The results indicate that the heat-induced decrease of f_{yx} [6] can be distinguished clearly only when the segment is longer than 120 cm. We also confirmed that the heat-induced BFS increment is observable if the segment is longer than 12 cm.

The distributed measurement ability is verified as demonstrated in Fig. 4. Four heated segments cascaded along the PMF sample are prepared [see Fig. 4(a)]. For the distributed measurement, the modulation frequency f_m is scanned from 860 to 930 kHz with a step of ~100 Hz corresponding to 16 cm; the microwave frequency to SSBM and the y-polarized carrier frequency are ramp swept for the characterization of BGS and DGS, respectively. As an example, the detected distribution of BGS and DGS from ~2 to ~9 m is illustrated in Fig. 4(b). The initial DGS is not uniform along the fiber owing to the irregularity of the local birefringence introduced during the fiber fabrication. Figure 4(c) summarizes the measured ν_B and f_{yx} along the fiber sample when the heater (a hot plate) with $\Delta T = \sim 15$°C is turned off (solid-circle line) or turned on (open-triangle line); their differences between the heater's on–off states are also shown (solid-star line). The opposite responses of the ν_B and f_{yx} to ΔT can be clearly observed. We repeat characterizing both the ν_B and f_{yx} with our correlation-based system at a fixed FM f_m (fixed sensing location as well). The maximum errors are estimated as low as ±0.7 MHz for ν_B ±11 MHz for f_{yx}, corresponding to maximum discriminative errors as ~16 $\mu\varepsilon$ and ~0.3°C by considering their strain and temperature sensitivities [6].

In conclusion, we have demonstrated a correlation-based cw method to localize the Brillouin dynamic grating and to measure its distribution in the PMF. A

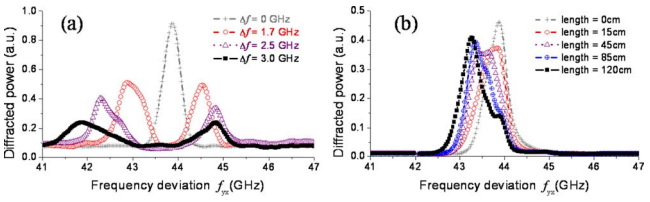

Fig. 3. (Color online) (a) Detected DGS for different FM modulation depths of DFB-LD1 when no FM is applied into DFB-LD2. (b) The detected DGS for a heated PMF segment localized at the correlation peak position but with different fiber lengths when FMs are synchronously applied to both DFB-LDs.

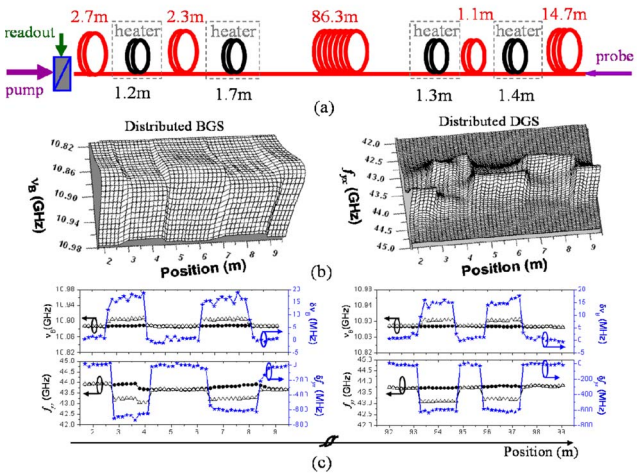

Fig. 4. (Color online) Distributed measurement results. (a) Prepared PMF sample. (b) Examples of 3D distribution of measured BGS and DGS from ~2 to ~9 m when the heater is turned on. (c) Summarization of detected BFS ν_B (upper) or frequency deviation f_{yx} (lower) and their temperature-induced changes near the heated segments. Solid-circle line (open-triangle line) corresponds to the heater being turned off (on); solid-star line indicates the temperature-induced changes between the heater's on–off states.

1.2 m spatial resolution and 110 m measurement range have been successfully realized. We believe ~10 cm order spatial resolution is expectable provided the availability of FM modulation depths and modulation frequency of laser sources. Further combination with our recent proposal of discrimination of strain and temperature by measuring both the ν_B and f_{yx} [6] will enable potential application in distributed and discriminative sensing for strain and temperature.

This work was supported by a "Grant-in-Aid for Creative Scientific Research" and the "Global Center of Excellence Program" from the Ministry of Education, Culture, Sports, Science and Technology, Japan.

References

1. K. Hotate and M. Tanaka, IEEE Photon. Technol. Lett. **14**, 179 (2002).
2. K. Y. Song, Z. He, and K. Hotate, Opt. Lett. **31**, 2526 (2006).
3. A. Fellay, L. Thevenaz, M. Facchini, M. Nikles, and P. Robert, in *Proceedings of International Conference on Optical Fiber Sensors* (1997) p. 324.
4. L. Zou, X. Bao, Y. Wan, and L. Chen, Opt. Lett. **30**, 370 (2005).
5. W. Zou, Z. He, and K. Hotate, J. Lightwave Technol. **26**, 1854 (2008).
6. W. Zou, Z. He, and K. Hotate, Opt. Express **17**, 1248 (2009).
7. K. Y. Song, W. Zou, Z. He, and K. Hotate, Opt. Lett. **33**, 926 (2008).
8. K. Hotate and T. Hasegawa, IEICE Trans. Electron. **E83-C**, 405 (2000).